PROCEEDINGS, 43rd Workshop on Geothermal Reservoir Engineering
Stanford University, Stanford, California, February 12-14, 2018
SGP-TR-213

Simulation of In-depth Water Diversion Using Sodium Silicate

R. Trujillo[1], D. Voskov[1,2], and O. Leeuwenburgh[1,3]

[1]Department of Geoscience & Engineering, TU Delft, Stevinweg 1, 2628 CN Delft, Netherlands
[2]Department of Energy Resources Engineering, Stanford University, Stanford, CA 94305, USA
[3]TNO, Princetonlaan 6, 3584 CB Utrecht, Netherlands

D.V.Voskov@tudelft.nl

Keywords: Sodium Silicate, In-Depth Water Diversion, Reactive Transport, Kinetic Reactions

ABSTRACT

In-depth water diversion is a chemical Enhanced Oil Recovery (EOR) method that has been gaining acceptance recently for several reasons. One of them is the fact that sodium silicate, used in this method, is one of the few green chemicals used in EOR. In addition, this chemical has shown the ability to generate thermally activated plugs far away from the wellbore and improve oil recovery due to the better sweep, as validated in several simulation studies and field pilots. In this work, we will apply this technique to extend the lifetime of geothermal doublets in simulations of low-enthalpy geothermal projects. The simulation model consists of a thermal-compositional reactive formulation that was implemented in Stanford's Automatic Differentiation General Purpose Research Simulator (ADGPRS) based on a fully implicit approach. The motivation for selecting this method is the strong coupling between chemical and flow variables linking the drastic changes in permeability induced by the reaction. The implementation of the silicate reaction assumes the oligomerization reaction proposed in Icopini et al. (2005) with kinetic rate suggested in Hiorth et al. (2016). This model describes the accumulation of solid silicate through a solid phase deposition and the resulting permeability changes due to pore blockage following a correlation described in Hiorth et al. (2016). We start with validation of the proposed model with an EOR case and obtain a close match to previous simulations as reported in Trujillo (2017). In this application, the model shows a successful generation of a plug around the middle of the reservoir, increased oil production rates after water breakthrough and an overall increase in cumulative oil production over 7%. Next, we apply the same model to a geothermal application where the generation of a plug helps to increase the time when the cold water is breaking through to the production well, thus extending the geothermal doublet lifetime. The plug placement has proven to be sensitive to different parameters such as the silicate concentration in the injected solution, the volume of the pre-flush batch and the total volumes of silicate solution injected. In addition, several numerical parameters, such as spatial and temporal resolution, can affect the accuracy of simulation results. In our study, we perform a sensitivity study to address these factors in typical hydrocarbon production and low-enthalpy geothermal projects.

1. INTRODUCTION

The growing demand for affordable energy requires innovating methods to be applied for an advanced energy extraction. One of the innovative methods is in-depth water diversion which has been proposed quite recently for improvement of oil recovery from hydrocarbon fields. For its chemical nature, in-depth water diversion is classified as a chemical EOR method. It is based on the injection of materials designed to travel along the reservoir and get activated when meeting certain conditions (e.g. chemical or thermal). The most common application currently targets the improvement of oil recovery within a reservoir containing highly permeable paths. For this case, sodium silicate is injected into the reservoir where it travels until reacting and forming gels. In this state, it becomes an effective plug that can withstand large pressure gradients, diverting water to previously unswept zones within the reservoir. In the past, most alternatives aimed for the near wellbore zones. However, recent studies showed the potential of sodium silicate to generate effective plugs at distances far from the injector well (Skrettingland et al., 2016). Moreover, the research in this field has increased significantly since sodium silicate was classified as a green chemical in the PLONOR list (Hatzignatiou et al., 2015).

Significant in-depth water processes have been reported mainly in the North Sea with pilot wells in the Gullfaks field (Lund et al., 1993; Rolfsvg et al., 1996) and extensively later in the Snorre field by (Stavland et al., 2011; Skrettingland et al., 2012, 2014, 2016). Along with these field pilots, some experimental work has been documented gathering information on the chemical reactions, activation mechanisms and behavior at core scale. On the other hand, relatively fewer efforts have been documented on the simulation of this process with the main exceptions being the work by Skrettingland et al. (2014), Huseynov (2010) and Hiorth et al. (2016). For this reason, we believe that investing in research on simulation can bring valuable insight of the process. Literature referring to this topic reveals research opportunities in methodology, physics description and identification of the control parameters. For example, only loosely coupled or uncoupled simulation techniques have been tested. To improve the physical description an incorporation of interdependent variables is needed, and an identification of important control parameters is essential for effective optimization of the process.

This study proposes the following methodology. A fully implicit approximation is used to solve the coupled physics of this chemical-transport problem. The simulation approach follows the research line implemented at Stanford University in the Automatic

Differentiation General Purpose Research Simulator (ADGPRS) by Farshidi (2016). This implementation was consistently extended by Fucios (2017) to account for changes in porosity-permeability due to in-situ kerogen upgrading. The contribution to the methodology proposed in this paper refers to the adaptation and validation of the new porosity-permeability model with incorporated reactions for in-depth water divergence. The impact of the resolution of space and time discretization on simulation results is addressed via a sensitivity study, with the aim to clarify if extended precision is needed when compared to classical flow and transport problems. The in-depth diversion process at continuous scale, five-species reactions was implemented. The identification and quantification of the effects of changes in the control parameters are performed through a sensitivity study targeting effects on gel generated and oil recovery. The new simulation formulation was tested for synthetic models of practical interest including oil production from hydrocarbon reservoirs and heat production from low-enthalpy geothermal fields.

2. METHODOLOGY

2.1. Overall scheme

Chemical-compositional transport problems involve the solution of several PDE's, along with some algebraic equations. Most of the physics involve high nonlinearity originating from the chemical and compositional processes. The discretization schemes used in this work are central difference approximation with upstream weighting in space and backward Euler approximation in time (LeVeque, 2016). To solve the nonlinear problem, the iterative Newton method is used. The detailed description of the implementation can be found in Farshidi (2016) and Voskov et al. (2016).

2.2. Compositional transport discretization

Mass transport phenomena are described by a hyperbolic equation usually denoted as the Cauchy problem (LeVeque, 2016). Generally, these equations are not stiff like the parabolic equation (e.g. conductive heat flow), which is one reason why there is a tendency to use explicit rather than implicit methods. Nevertheless, since several equations will be solved simultaneously, implicit methods are preferred to avoid stability difficulties while choosing an appropriate timestep.

The mass conservation transport problem can be approached by two different methods: the natural variable formulation and the molar variable formulation (Cao, 2002; Voskov and Tchelepi, 2012). The latter has been selected for this work because of the reduced number of unknown variables which translate to a simpler Jacobian construction (Voskov and Tchelepi, 2012). Furthermore, the description of compositional changes is simplified by means of a K-values formulation, where each value has been defined a priory from equilibrium conditions.

The method follows the research line implemented in the Automatic Differentiation General Purpose Research Simulator (ADGPRS) using an overall composition formulation (Voskov and Tchelepi, 2012). Under this framework, the mass conservation over a control volume including an accumulation term A, a flux term F and a source term S is:

$$A + F + S = 0 \tag{1}$$

$$\frac{d}{dt}(\phi \rho_T Z_i) + \nabla \cdot \sum_{j=1}^{n_p} (\rho_j X_{ij} \vec{u}_j) + \sum_{j=1}^{n_p} \rho_j X_{ij} q_j = 0 \tag{2}$$

$$V\left[(\phi \rho_T Z_i)^{n+1} - (\phi \rho_T Z_i)^n\right] - \Delta t \sum_l \left(\sum_{j=1}^{n_p} x_{ij}^l \rho_j^l \Gamma_j^l \Delta \psi^l \right) + \Delta t \left(\sum_{j=1}^{n_p} x_{ij} \rho_j q_j \right) = 0 \tag{3}$$

In equation 3, $\vec{u}_j$ represents the Darcy's phase velocity. Additionally, we use a two-point flux approximation with upstream weighting where $\Delta\psi^l$ is a pressure potential over an interface l and Γ^l corresponds to the transmissibility (Khait and Voskov, 2017). Note that the approximation for transmissibility is separated into two parts. The first (geometric) term treats absolute permeability and block properties. The second term includes fluid properties. The approximation for the geometric part is performed by harmonic averaging. The fluid property term is approximated using upstream weighting (Aziz and Durlovsky, 2013). A system of mass conservation is closed using various algebraic constraints and thermodynamic equilibrium assumption, see details in Voskov and Tchelepi (2012).

2.3. Chemical transport discretization

Reactions can take place in both fluid species and solid (gel) species. This study assumes that the solid species are not transported. As a consequence, they are deposited in the matrix changing the porosity. Therefore, the reactive transport mass conservation of liquids and solids components is:

$$A + F + S + R = 0 \tag{4}$$

This equation can be written for liquid components

$$\frac{d}{dt}(\phi\rho_T Z_i) + \nabla \cdot \sum_{j=1}^{n_p}(\rho_j X_{ij}\vec{u}_j) + \sum_{j=1}^{n_p}\rho_j X_{ij} q_j + \sum_{k=1}^{n_k} v_{ik} r_k + \sum_{q=1}^{n_q} v_{iq} r_q = 0 \tag{5}$$

and for solid components

$$\frac{d}{dt}C_m = \sum_{k=1}^{n_k} v_{ik} r_k + \sum_{q=1}^{n_q} v_{iq} r_q. \tag{6}$$

In these equations, the suffix k represents the kinetic reactions and q represents the equilibrium reactions. The variable C_m is the concentration of solids represents the deposition of this specie due to a chemical reaction. Following Khait and Voskov (2017), we neglect all the equilibrium reactions and impose the assumptions of compositional transport, the equations for liquid components can be discretized as follows:

$$V\left[(\phi\rho_T Z_i)^{n+1} - (\phi\rho_T Z_i)^n\right] - \Delta t \sum_l \left(\sum_{j=1}^{n_p}\rho_j^l X_{ij}^l \Gamma_j^l \Delta\psi^l\right) + \Delta t\left(\sum_{j=1}^{n_p}\rho_j X_{ij} q_j\right) + \Delta t\left(\sum_{k=1}^{n_k} v_{ik} r_k\right) = 0 \tag{7}$$

and for solid components as

$$V\left[(C_m)_i^{n+1} - (C_m)_i^n\right] + \Delta t\left(\sum_{k=1}^{n_k} v_{ik} r_k\right) = 0 \tag{8}$$

2.4. Energy equation discretization

According to Khait and Voskov (2017), the thermal equation can be discretized for an unstructured grid and a backward Euler approximation in time in the following way:

$$\begin{aligned} V\left[\left(\phi\sum_{j=1}^{n_p} S_j\rho_j U_j + (1-\phi)U_r\right)^{n+1} - \left(\phi\sum_{j=1}^{n_p} S_j\rho_j U_j + (1-\phi)U_r\right)^{n}\right] \\ -\Delta t\sum_l\left(\sum_{j=1}^{n_p} h_j^l\rho_j^l\Gamma_j^l\Delta\psi^l + \Gamma_c^l\Delta T^l\right) + \Delta t\left(\sum_{j=1}^{n_p} h_j\rho_j q_j + q_h\right) = 0 \end{aligned} \tag{9}$$

In the previous equation, we use a two-point flux approximation with upstream weighting where $\delta\psi^l$ is a pressure potential over an interface l, ΔT^l is a difference in temperature over neighboring blocks, Γ_j^l corresponds to the phase transmissibility including permeability and geometry, and Γ_c^l presents the conductive transmissibility including the thermal conduction of all phases and the geometric part.

2.5. Chemical models

In addition to the regular transport models, in-depth water diversion requires additional information on how to build the chemical reactions and how to generate the permeability changes. The reaction for silica gelation proposed by Icopini et al. (2015) is used since they are considered to be a more accurate representation of the overall process.

$$H_8Si_3O_{10(\mathrm{aq})} + H_4SiO_{4(\mathrm{aq})} \xrightarrow{k_1} H_8Si_4O_{12(\mathrm{gel})} + 2H_2O$$
$$4 \text{ components reaction} \tag{10}$$

According to Icopini et al (2015), the reaction rate k in the silica polymerization process is driven by the consumption of the monomer H_4SiO_4 denoted by a power 4 relation of the changes in concentration as follows:

$$\frac{d[H_4SiO_{4(aq)}]}{dt} = -k[H_4SiO_{4(aq)}]^4 \tag{11}$$

A permeability relation based on a pore throat blockage presented by Hiorth et al. (2016) is selected since it was observed to be a better approximation of the process during large-scale simulations (Trujillo, 2017).

$$Permeability(si) = k_o \left(1 + 275 Y S_w \sqrt[2]{\frac{k_o}{\phi_o}}\right)^{-2} \tag{12}$$

In this equation, k_o represents the initial permeability and Y the mass fraction of deposited silicate over the mass of water.

The change of porosity is related to the molar deposition of the solid species as follows:

$$\phi(t) = 1 - C_{rock} - \frac{N_{solid}(t) \times M_{v_{solid}}}{V_{cell}} \tag{13}$$

Here, C_{rock} represents the fraction of volume corresponding to rock which remains unchanged in time, N_{solids} is the number of moles of solid species deposited and M_{vsolid} is the molecular volume of the solid in [$m^3/moles$].

3. SIMULATION RESULTS

3.1. Resolution study

The spatial and temporal discretizations required for accurate representation of subsurface transport phenomena have been extensively studied. Typically, convergence of the solution can be achieved with grid blocks of several tenths of meters and simulation steps in the order of weeks or even months. However, transport and kinetics are phenomena involving very different time and space scales. From the governing equations 2 and 11, it is noticed that the transport equation is a global equation (due to the flux term) while kinetics are purely local. It is known that problems involving chemical kinetics include physics that occur at different scales than regular transport ones. The chemical process usually involves physics taking place in a local domain and occurring much faster than transport. To determine a proper scale over which a converged solution can be assumed, a time-space convergence study is implemented below. The study is performed for a 1D subsurface over which the thermal-compositional reactive formulation is implemented. Description of the subsurface is provided in Appendix A.

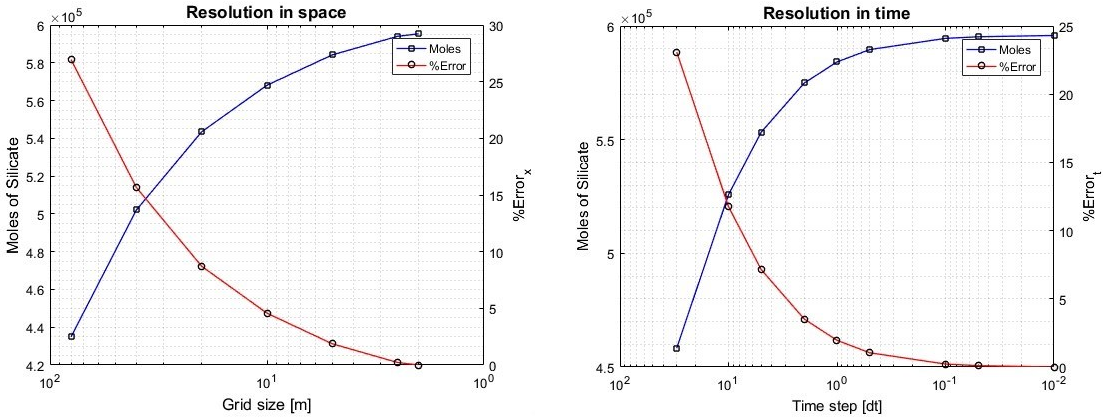

Figure 1: ***Space and time resolution for 1D simulation with the kinetic rate from the fourth model***

By gradually increasing the resolution in space and time, the solution converges at relatively fine values, below 1 meter in space and close to 0.1 days in time. These magnitudes are much lower than the values used for regular simulations at reservoir scale. Because of computational time limitations, very high-resolution models are not viable for 2D and 3D problems. Therefore, a time step ranging from 1 to 2 days, giving an error below 3% compared to the converged solution, seems appropriate for large-scale models. Likewise, for the spatial domain, a grid with a characteristic size of 5m in the flow direction also produces an error below 3% and is appropriate for a multi-dimensional simulation.

3.2. Calibration of the reaction rate

One of the key parameters of the process is the reaction rate. This variable is an important driver of the chemical module and requires calibration since literature data from experiments differ from the typical simulation conditions. This parameter includes information from the thermal and chemical mixture terms as follows:

$$k = \frac{1}{a\xi e^{\beta[HCL]} e^{\gamma\sqrt{[Ca]}} e^{\frac{E_a}{RT}}} \qquad k = k_o e^{\frac{-E_a}{RT}} \tag{14}$$

The thermal part is represented by the Arrhenius equation while the purely chemical term will be denoted k_o. From now on, calibration of the reaction rate will refer only to the chemical term k_o, called normalized reaction rate ($k_o = k/e^{-Ea/RT}$). In their work, Icopini et al. (2005) and Hiorth et al. (2016), propose two different ranges for this parameter:

Normalized reaction rate k_o $[mol/m^3]^{-1} \cdot s^{-1}$	
Icopini	Hiort
$2 \cdot 10^4$ - $6 \cdot 10^7$	$1 \cdot 10^{12}$

Table 1: Reaction rates from experiments in bulk at 25° for concentrations of 0.16w% silicate in Icopini's and 4w% silicate in Hiorth's experiments.

Calibration of this parameter over a 1D homogeneous idealized reservoir (see appendix A) with the corresponding model described in 2.5 for the injection of 4w% silicate results in:

Normalized reaction rate	
k_{rxn} $[mol/m^3]^{-1} \cdot s^{-1}$	Silicate volume $[m^3]$
$4.0 \cdot 10^6$	150

Table 2: Normalized reaction rates that create a blockage for each model

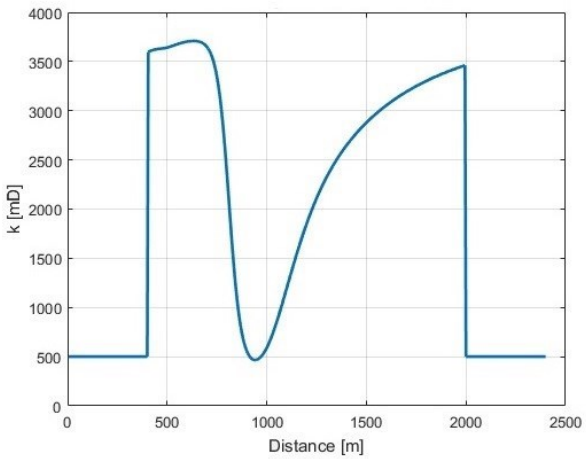

Figure 2: Permeability profile distribution.

From table 2, it is noticed that the calibrated value for the reaction rate falls within the experimental data proposed by Icopini et al. (2015). This study allows the first approximation between experimental data and simulation, an idea further developed in Trujillo

(2017). From the figure 2, it is noticed that the model generates a major reduction in the original permeability profile from 4000 md to 500 md located at 900 meters, approximately 500 meters from the injector well. This permeability reduction is considered to be strong enough to allow water diversion from the high permeability regions to the lower ones. These results suggest that the use of a permeability reduction model from equation 12 is appropriate for simulation of flow diversion processes. For this reason, it will be used for further multi-dimensional simulations. It is important to notice that a small permeability reduction takes place up to about 200-300 meters from the well. This reduction represents a change of 7% suggesting an opportunity to apply optimization techniques in order to decrease this value.

3.3. Sensitivity to reaction rate

The reaction rate has proven to be a complex parameter. Because of this, a sensitivity study of its variations is presented below. The study considers the effects over two critical variables by varying this parameter. the variables are the moles of solids produced and the permeability reduction. In the following graph, changes in these two variables are presented due to the effect of varying the reaction rate up to ±50%.

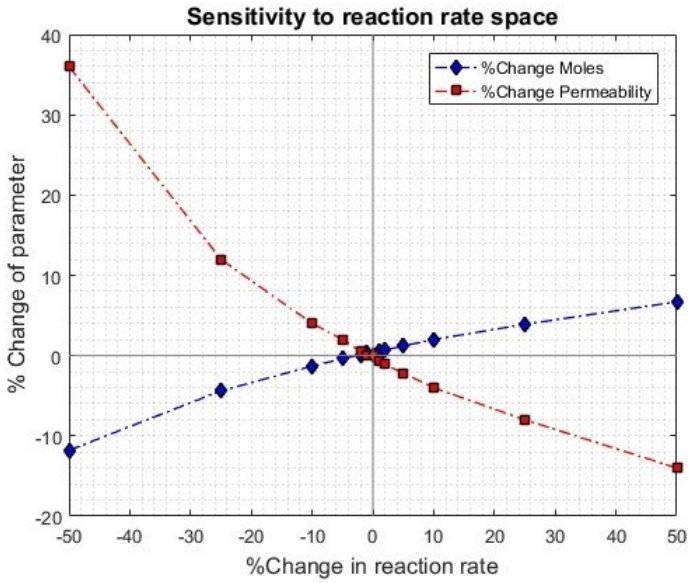

Figure 3: Reaction rate sensitivity to changes in parameters

From figures 3, it is noticed that the variation in the moles of solid silicate is not very significant and almost linear. On the other hand, the variations in permeability are considerable, showing high nonlinearities when the reaction rate is reduced. For instance, having in mind the wide range for the reaction rate proposed by Hiorth et al. (2016) in table 1, a miscalculation in this parameter would lead to important changes in permeability, and therefore, significant variations in the flow pattern.

3.4. Water diversion in 2D

A water diversion simulation is presented for the 2D reservoir described in Appendix A. For the following injection schedule over a total of 2000 days period, the results on permeability profile modification, water saturation, and heat diversion are presented below.

Silicate injection	
Period [days]	Molar fraction (Z)
420	1 H_2O
200	0.01 Si
1380	1 H_2O

Table 3: Injection schedule for 4% silicate solution

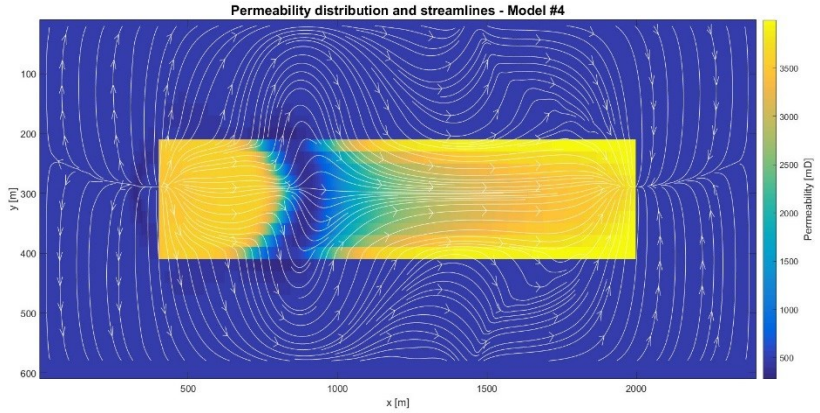

Figure 4: Permeability and streamlines distributions

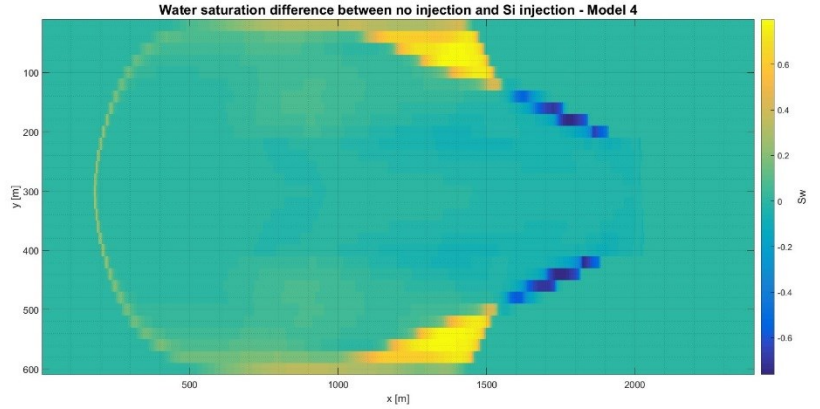

Figure 5: Water saturation profiles difference. Sw of silicate minus Sw without silicate.

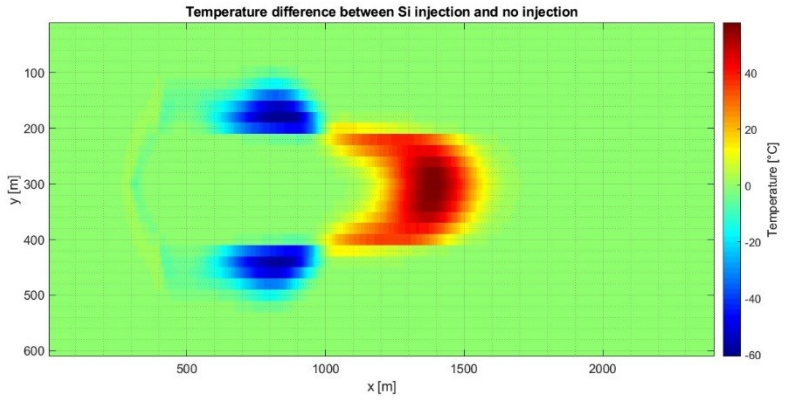

Figure 6: Temperature profiles difference. Temp. of silicate minus Temp. without silicate.

From figure 4, it is observed that the model creates an effective blockage causing water to divert to the low-permeable zone. The plug size is about 200 meters long, spreading over the entire width of the high-permeable channel. The permeability in this section has been reduced from the original 4000 md to an average of 260 md. Deposition of mineral silicate is also observed in small areas outside the main channel. As shown by the streamlines in the same figure, the water has been diverted to lower-permeability zones giving a better sweep in these areas.

The water saturation distribution in figure 5 displays two important facts. First, the recovery in the far extremes of the reservoir is largely improved with water saturation close to 0.9. Second, a clear stable waterfront is created after crossing the plug which is an indication of a better sweep efficiency. The effects over the production due to water diversion account for an increment of 6% during the simulation period of 2000 days as reported by Trujillo (2017).

From figure 6, it is noticed that, after the silicate injection, additional heat is recovered from the water diversion around the plug. This is noted by the two blue lobes located at around 800 meters which represent parts of the reservoir that have been cooled down. Moreover, the region in red illustrates a new thermal front moving towards the producer at approximately 40 degrees Kelvin warmer than in the case without silicate injection. While additional heat production is not affecting directly the produced oil, this effect is very important in low-enthalpy geothermal processes where heat production is a primary goal.

3.5. Sensitivity of 2D results

Since a 2D model gives further inside about the water diversion process, 3 control parameters where identified and studied. The parameters are silicate concentration in the mixture, the volume of silicate mixture injected, and water batch used prior to the silicate injection. Its effect on the process was quantified by the variation in the produced oil and a generated volume of solid (gel).

Overall, the variation of total oil produced in all cases is quite moderate. Even the maximum variation of the parameters in ±50% won't produce more than 2.5% difference in the additional recovery ($2.23 \times 106to2.17 \times 106m3$). It is worth mentioning that the variations were obtained for each parameter independently. A correlated variation of parameters could lead to further oil recovered. Moreover, even a small variation over the total oil recovery is economically valuable. Just a couple of percentage points over the base case (parameters from table 3) usually mean that costs are recovered, and extra revenues are obtained.

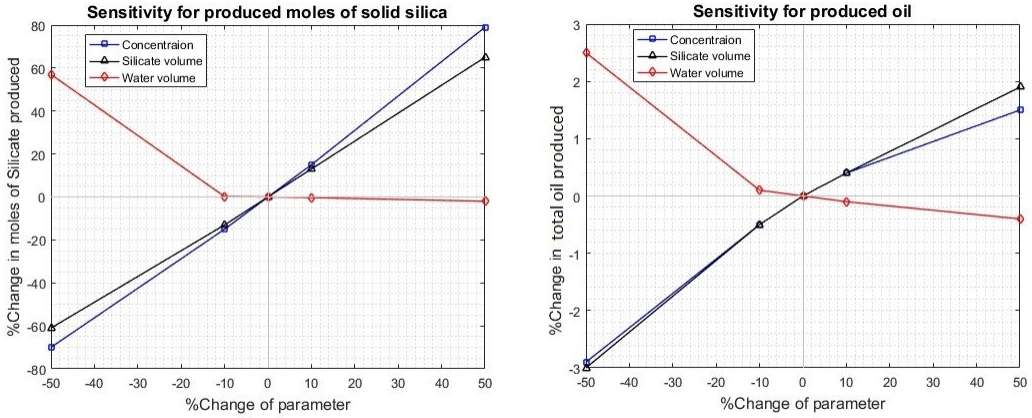

Figure 7: Sensitivity to changes in parameters a. silicate moles produced. b. Cumulative production.

3.6. Geothermal application

For the geothermal application, the purpose of the water diversion process is to create a blockage to delay the reduction in temperature of the production fluids. In principle, if water is diverted to unswept zones, the injection fluids will be in contact with the hot reservoir rock for a longer period. Therefore, by deviating from the main channels, the fluid will gain additional energy from reservoir rock and the thermal breakthrough will be delayed.

For this geothermal application, a single layer of a low enthalpy reservoir typical for Western Netherlands and suggested in Willems (2017) and Shetty (2017) was modeled with a permeability contrast of 4000 md for the channels and 500 md for the floodplain.

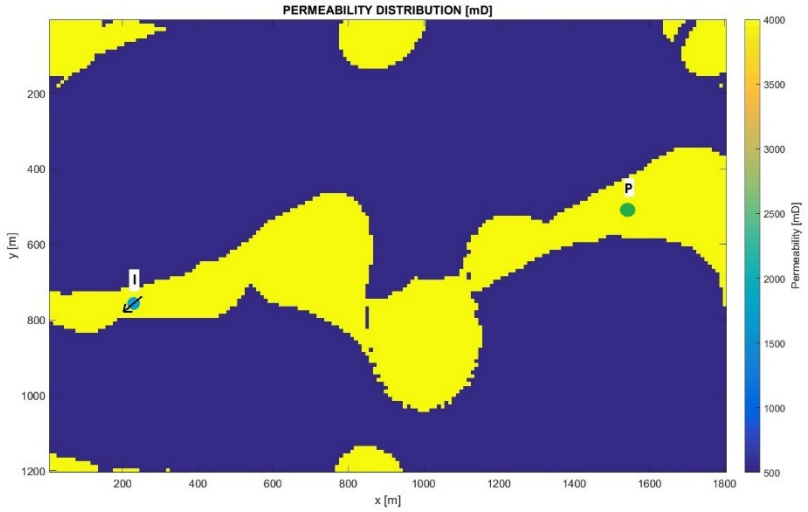

Figure 8: Permeability profile for geothermal doublet.

According to Willems (2017), the geothermal well doublet stops being economical if the temperature of the produced fluids drops by 10 degrees from the original fluids. When this condition is achieved, the production well is shut down.

The injection schedule for the simulation of silicate injection is presented below. The injector is operated at a constant rate of 100 [m3/day]. This value is scaled according to the ratio between the original reservoir thickness and the thickness of the layer modeled in this study. The temperature profile for the produced fluids over 35 years is presented in figure 9.

Without silicate injection		**Silicate injection**	
Period [years]	Molar fraction (Z)	Period [years]	Molar fraction (Z)
		4.1	1 H_2O
35	1 H_2O	1.4	0.01 Si
		29.5	1 H_2O

Table 4: Injection schedule geothermal doublet.

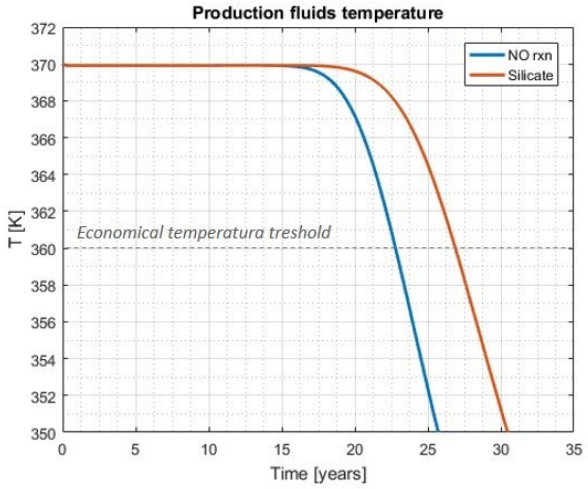

Figure 9: Production's fluids temperature without and with silicate injection.

From the figure 9, it can be observed that for the base case (in blue) the temperature starts decreasing after 16 years of production. Beyond this point, a sharp decline is noticed. In this scenario, the geothermal doublet reaches its lifetime according to the economic conditions after 22 years of production, when the temperature drops 10 degrees to a value of 360 K. For the silicate injection case (red line), the temperature starts declining only after 20 years of production. Moreover, the temperature decline has a smaller slope. In this scenario, the geothermal doublet will reach its economic lifetime after 26.5 years of production when the temperature reaches the mentioned threshold. More insight of the thermal difference can be obtained from figure 10.

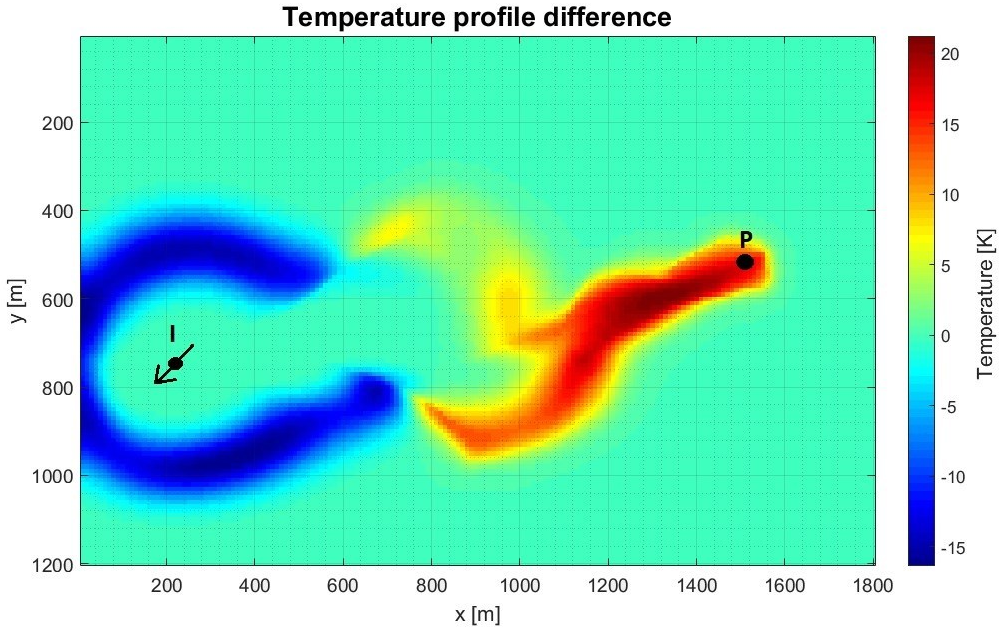

Figure 10: Thermal profile difference for silicate injection and base case at year 25.

The reservoir temperature difference (silicate case minus base case) after 25 years of production helps to visualize where the heat contributions are coming from. An additional cooling can be observed in the low permeability regions outside the channel near the injector well. Some additional heat is observed reaching the production well, explaining the temperature difference of 12 degrees in figure. 9.

In this geothermal application, injection of silicate creates changes in permeability profile that divert water. As consequence, water flows outside the high-permeable path and the fluids reach still warm zones of the reservoir thus increasing the produced fluid temperature. As a result, water diversion by injection of sodium silicate delays the thermal breakthrough extending the lifetime of the geothermal doublet.

4. SUMMARY AND DISCUSSIONS

Results of silicate injection for EOR in an idealized reservoir demonstrated that the process can generate substantial permeability variation after which water diverts to unswept low-permeability regions. The flow patterns and thermal activation of the reaction in this study indicate a significant coupling between flow, mass transport, energy and chemical reaction. That advocates an implementation of a fully-implicit coupling to model this process. The geothermal application shows how the water diversion process can be used to modify thermal profiles in the same way as is done for the purpose of increasing oil recovery. This process enabled a delay in thermal breakthrough time of several years in a 2D example. Moreover, the temperature of the production fluids was maintained above the economic threshold for 5 additional years leading to an extended geothermal doublet lifetime. These findings encourage an extensive study of this application as this approach is novel in geothermal industry.

Silica polymerization is a complex process worthy of further research. A major difficulty is how to describe particle growth from monomers to polymers in a chemical reaction. The current model gives satisfactory results. However, the particle enlargement, which plays a major role in in-depth diversion, could be further represented by integrating reactions that account for later stages of polymerization and particle size growth. In the same line of thought, the permeability model driven by pore throat blockage proved to be appropriate for this study. This formulation relates the surface area of the deposited solids to the area of the pore throats. Therefore, it allows smaller porosity reductions to generate significant permeability modifications. Even though this kind of relations seems to be appropriate, the model could be further tuned for a specific particles size in future studies.

Addressing kinetics, the sensitivity study for space and time discretization confirms the need for a higher resolution when modeling fast changing and localized process as silicate gelation kinetics. More precisely, grid sizes of 1 meter along the flow with 0.1 day time steps are suggested to reach the numerically converged solution. This resolution is highly demanding on computational power, but these values can be relaxed if small errors in the solution are acceptable. In summary, given that the possible improvements in oil recovery and extension of the geothermal doublet lifetime are economically attractive, the implementation of an in-depth water diversion process in the two applications shows a great potential.

REFERENCES

Aziz, K., Durlofsky, L.: Notes on Reservoir Simulation. Energy Resources Engineering. Stanford university (2013).

Cao, H.: Development of techniques for general purpose simulators. Doctor of Philosophy dissertation. Stanford University (2002).

De Hoop S.: Determination of Relevant Spatial Scale in Reservoir Simulation. Master thesis. Department of Applied Earth Science. Delft University of Technology (2017).

Fan, Y.: Chemical reaction modeling in a subsurface flow simulator with application to in-situ upgrading and CO2 mineralization. Doctor of Philosophy dissertation. Stanford University (2010).

Farshidi, S.: Compositional reservoir simulation-based reactive-transport formulation, with application to cO2 storage in sandstone and ultramafic formations. Doctor of Philosophy dissertation. Stanford University (2016).

Fuciños, R.: Hierarchical coarsening of simulation model for in-situ upgrading process. M.Sc. thesis. Department of Applied Earth Science. Delft University of Technology (2017).

Hatzignatiou, D., Giske, N.: Water-Soluble Sodium Silicate Gelants for Water Management in Naturally Fractured Carbonate Reservoirs. SPE-180128, (2016).

Hiorth, A., Sagen, J., Lohne, A., Nossen, J., Vinningland, J.L., Jettestuen, E., and Sira, T.: IORSim - A Simulator for Fast and Accurate Simulation of Multi-phase Geochemical Interactions at the Field Scale. EAGE ACMOR XV 10.3997/2214-4609.201601882, (2016).

Huseynov, R.: Silicate modeling and experimental study for deep water Diversion in IOR. Master thesis. Department of Applied Earth Science. Delft University of Technology (2010).

Icopini, G., Brantley, S.L., and Heaney, P.J.: "Kinetics of Silica oligomerization and nanocolloid formation as a function of pH and ionic strength at 25∘C", Geochimica et Cosmochimica Acta 69, (2005), 293-303, 10.1016/j.gca.2004.06.038.

Iler, R.: The chemistry of silica: Solubility, polymerization, colloid and surface properties, and biochemistry (A wiley-Interscience publication). New York: Wiley (1979).

Jurinak, J., Summers, L., Bennett, K.E.: Laboratory testing of Colloidal Silica Gel for Oilfield Applications. SPE 23581 (1991).

Khait, M., Voskov, D.: Operator-based linearization for general purpose reservoir simulation. ELSEVIER - Journal of Petroleum Science and Engineering (2017).

Krumrine, P., Boyce, S.: Profile Modification and Water Control With Silica based Systems. SPE 13578, (1985).

Lake, L., and Society of Petroleum Engineers of AIME.: Fundamentals of enhanced oil recovery ([2nd ed.]. ed.). Richardson, Tex.: Society of Petroleum Engineers (2014).

LeVeque, R.: Numerical methods for conservation laws (2nd ed. ed., Lectures in mathematics ETH Zurich). Basel: Birkhauser (2006).

Lichtner, P., Steefel, C., and Eric H., Editors. Reactive Transport in Porous Media. Reviews in Mineralogy Volume 34, (1996).

Lund, T., Kristensen, R.: Qualification program for deep penetration gels: From laboratory to Field. IEA symposium on EOR. Salzburg, Austria (1993).

Oran, E., and Boris, J.: Numerical simulation of reactive flow (2nd ed. ed.). Cambridge, U.K.: Cambridge University Press (2001).

Pietro, A., Jimenez, J., Tabuteau, H., Turuban, R., Borgne, T., Derrien, M., and Méheust, Y.: Mixing and reaction kinetics in porous media: an experimental pore scale quantification. Université de Rennes. Rennes. France.

Rolfsvåg, T., Jakobsen, S., Stromsvik, G.: Thin Gel treatment of an Oil producer at the Gullfaks field: Results and Evaluation. SPE 35548, (1996).

Schäfer, M.: Computational engineering: Introduction to numerical methods. Berlin. Springer (2006).

Shetty, S.: Numerical strategy for uncertainty quantification in low-enthalpy geothermal projects. M.Sc. thesis. Department of Applied Earth Science. Delft University of Technology (2017).

Skrettingland, K. et al.: Snorre In-Depth water Diversion Using Sodium Silicate - Single Well Injection Pilot. SPE 154004, (2012).

Skrettingland, K. et al.: Snorre In-Depth Water Diversion Using Sodium Silicate - Large Scale Interwell Field Pilot. SPE 169727, (2014).

Skrettingland, K. et al.: Snorre In-Depth water Diversion - New Operational Concept for Large Scale Chemical Injection from a Shuttle Tanker. SPE 179602, (2016).

Stavland, S., Jonsbråten, H.C., Vikane, O., Skrettingland, K., and Fischer, H.: In-Depth water diversion using sodium silicate on Snorre - Factors controlling In-Depth placement. SPE 143836, (2011).

Trujillo, R.: In-Depth Water Diversion Simulation Strategies. M.Sc. thesis. Department of Applied Earth Science. Delft University of Technology (2017).

Vinot, B., Schecter, R., Lake, L.: Formation of Water-Soluble Silicate Gel by Hydrolysis of a Diester of Dicarboxylic Acid Solubilized as Microemulsion. SPE 14236, (1985).

Voskov, D., Tchelepi, H.: Comparison of nonlinear formulations for two-phase multi-component EoS based simulation. In Journal of Petroleum Science and Engineering, Volumes 8283, (2012), Pages 101 - 111, ISSN 0920-4105.

Voskov, D., Henley, H., and Lucia, A.: Fully compositional multi-scale reservoir simulation of various co2 sequestration mechanisms. Computers and Chemical Engineering (2016).

Willems, C.: Doublet deployment strategies for geothermal Hot Sedimentary Aquifer exploitation. Doctor of Philosophy dissertation. Department of Applied Earth Science. Delft University of Technology (2017).

APPENDIX A: Description of homogeneous model

For a 1D and 2D homogeneous reservoir case, the chemical species description is shown in table 5. The Corey relative permeability parameters are specified in table 6. The rock parameters as specified in table 7. The well placement for this scenario is given in table 8. The fluids phase properties are detailed in table 9. The reservoir geometry follows parameters defined in table 10.

Reaction's species			
C1	Oil	*Decane*	142 [gr/mol]
C2	Water		18 [gr/mol]
C3	H_4SiO_3	*Aqueous Silicate*	96.1 [gr/mol]
C4	$H_8Si_3O_{10}$	*Aqueous Silicate*	252.3 [gr/mol]
S1	$H_8Si_4O_{12}$	*Gel Silicate*	156 [cm^3/mol]
k		*reaction rate*	$4 \cdot 10^6$ [mol/m^3]$^{-1} \cdot s^{-1}$

Table 5: Reacting species

Corey relative permeability	
n_w	2
S_{rw}	0.081
k_{rw}	1
n_o	3
S_{rw}	0

Table 6: Corey relative permeability parameters

Rock description		
ϕ	0.3	
k	4000 or 500	$[md]$
Compressibility	$1e^5$	$[1/bar]$
Specific heat capacity	3000	$[kJ/kg \cdot K]$
Thermal conductivity	$1e^2$	$[kJ/m \cdot day \cdot k]$

Table 7: Rock properties

Well placement			
Well	X $[m]$	Y $[m]$	Perforation in Z $[m]$
Producer	405	300	4030 - 4040
Injector	1995	300	4030 - 4040

Table 8: Well coordinates

Phases description		
OIL		
ρ_o	0.8	$[gr/cm^3]$
μ_o	1	$[cP]$
Liquid heat capacity coefficients in $[J/g \cdot mol \cdot K^n]$		
GPL1	-7.913	
GPL2	0.9609	
GPL3	0.9609	
GPL4	1.131e-7	
Vaporization enthalpy		
HVR	5579	$[J/g \cdot mol \cdot K^{ev}]$
Heat conductivity		
THC	13	$[kJ/m \cdot day \cdot K]$

WATER		
ρ_w	1	$[gr/cm^3]$
μ_w	1	$[cP]$
Liquid heat capacity coefficients in $[J/g \cdot mol \cdot K^n]$		
GPL1	32.243	
GPL2	1.924e-3	
GPL3	1.055e-5	
GPL4	-3.596e-9	
Vaporization enthalpy		
HVR	4820	$[J/g \cdot mol \cdot K^{ev}]$
Heat conductivity		
THC	58	$[kJ/m \cdot day \cdot K]$

Table 9: Phase properties

Reservoir description		
x	2400	$[m]$
y	600	$[m]$
z	70	$[m]$
Cells in x	480	-
Cells in y	30	-
Cells in z	7	-
Depth	4000	$[m]$
Pressure	400	$[m]$
Temperature	370	$[K]$

Table 10: Reservoir parameters

APPENDIX B: Description of geothermal model

For the 2D geothermal case, the chemical species description is shown in table 5. The rock parameters are following table 7. The fluid phase description is as detailed in table 9. The reservoir geometry is specified in table 11. The well placement for this case goes according to table 12.

Reservoir description		
x	1800	$[m]$
y	1200	$[m]$
z	10	$[m]$
Cell in x	180	-
Cell in y	120	-
Cell in z	1	-
Depth	4000	$[m]$
Pressure	400	$[m]$
Temperature	370	$[K]$

Table 11: Geothermal reservoir parameters

Well placement		
Well	X $[m]$	Y $[m]$
Producer	1550	500
Injector	210	760

Table 12: Well coordinates geothermal